Hindawi Publishing Corporation
International Journal of Antennas and Propagation
Volume 2015, Article ID 895963, 7 pages
http://dx.doi.org/10.1155/2015/895963

Research Article

Design of a Circularly Polarized Galileo E6-Band Textile Antenna by Dedicated Multiobjective Constrained Pareto Optimization

Arnaut Dierck,[1] Frederick Declercq,[1] Thomas Vervust,[2] and Hendrik Rogier[1]

[1]*Electromagnetics Group, Department of Information Technology, iMinds-Ghent University, 9000 Ghent, Belgium*
[2]*Centre for Microsystems Technology, IMEC-Ghent University, 9000 Ghent, Belgium*

Correspondence should be addressed to Arnaut Dierck; arnaut.dierck@intec.ugent.be

Received 28 July 2014; Revised 17 November 2014; Accepted 18 November 2014

Academic Editor: Diego Caratelli

Designing textile antennas for real-life applications requires a design strategy that is able to produce antennas that are optimized over a wide bandwidth for often conflicting characteristics, such as impedance matching, axial ratio, efficiency, and gain, and, moreover, that is able to account for the variations that apply for the characteristics of the unconventional materials used in smart textile systems. In this paper, such a strategy, incorporating a multiobjective constrained Pareto optimization, is presented and applied to the design of a Galileo E6-band antenna with optimal return loss and wide-band axial ratio characteristics. Subsequently, different prototypes of the optimized antenna are fabricated and measured to validate the proposed design strategy.

1. Introduction

With the advent of ubiquitous computing, the need for ever smaller, cheaper, and more powerful electronic devices has increased significantly. Smart fabrics and interactive textiles (SFIT) offer great potential to increase the functionality in a wide gamut of applications at a low cost, both in terms of price and space. From healthcare to civil services, by using suitable materials such as (conductive) textiles, foams, and 3D fabrics to realize active circuits and antennas, electronic systems can be unobtrusively integrated into clothing, implementing features that would otherwise require additional, often cumbersome, devices that have to be carried around [1–8]. For rescue workers, having access to services such as positioning, victim localization, vital signs monitoring, and environmental hazard sensing can mean the difference between life and death. Replacing the traditional, rigid, hand-held devices by electronics directly integrated into the wearer's garment, however, does not come without specific design challenges. The placement of the wearable systems inside of a garment makes them susceptible to influences of the proximity of the body. Moreover, the foam and fabric substrates give rise to additional losses and their flexibility, while being indispensable for a conformal integration into clothing makes the antennas vulnerable to bending, potentially affecting their performance [9, 10]. Additionally, the off-the-shelf foam/textile materials, which have not been specifically designed and fabricated as radio frequency (RF) substrates, can exhibit high variations on their RF properties when looking at different product batches. These variations can cause an unwanted shift in the antenna frequency response, which can reduce performance in the required frequency range. As wearable applications often require a low-profile antenna, the antenna thickness, mainly determined by the height of the antenna substrate, is a key aspect in the design process. A thinner antenna substrate offers a more comfortable integration into the garment but, at the same time, limits the margins the designer can introduce to ruggedize the antenna to material variations by increasing the antenna bandwidth. In order to meet the stringent requirements for modern applications, in terms of both performance and wearability, it is important not only to base the design on a suitable antenna topology that is subsequently optimized in view of the different design objectives, but also

to be able to cope with the potentially large variations of the used foam/textile materials.

Aperture-coupled circularly polarized patch antennas provide a versatile topology for wearable, robust user-terminal antennas for satellite communications [1, 2]. The intricate effect of the different design parameters on the antenna performance, combined with the variations on the applied substrate materials, demands a dedicated design strategy, employing a multiobjective optimization approach in tandem with a final postoptimization step to accommodate for potential variations in the foam/textile substrates. Multiobjective optimization has been successfully applied to several areas of electromagnetic design, such as antennas [11, 12], antenna arrays [13, 14], and filters [15, 16]. Here, we propose a novel dedicated textile antenna design strategy applied to a Galileo E6-band antenna. The method is based on a multiobjective constrained Pareto optimization that is able to combine resources from suitable simulators and databases to achieve a design that is jointly optimized for different, often conflicting, objectives, followed by a final postoptimization to accommodate for unexpected deviations in the substrate characteristics. The presented Galileo E6-band antenna takes as a starting point the GPS E1-Iridium antenna topology presented in [1], which is then optimized in terms of wearability, by applying a substrate that is almost 50% thinner and a significantly smaller discrete hybrid coupler. Despite the reduced thickness of the antenna substrate, the Galileo E6-band antenna has to cover a frequency range from 1.26 to 1.3 GHz, which amounts to a fractional bandwidth of 3.1%, hardly less than the fractional bandwidth of 3.3% that is covered by the GPS-Iridium antenna. Therefore, to enhance the antenna for Galileo E6-band reception, the feed circuit has been redesigned. This large bandwidth, required in terms of both antenna impedance and axial ratio, poses a heavy challenge, especially for circular polarization of the antenna. Indeed, in [17] it is stated that conventional single-feed designs [18] on thick substrates achieve simultaneous impedance and AR bandwidth between 1% and 2%. To cover the complete Galileo E6-band, a simultaneous impedance/AR bandwidth of at least 3.1% is required. Moreover, a low-profile textile antenna is needed, in order to avoid compromising its wearability. Reference [17] realizes a bandwidth of 12.6%, albeit on a 10 mm thick substrate at 2.45 GHz, corresponding with $d/\lambda = 8\%$. In our paper, the antenna covers the 3.1% bandwidth with a 3.94 mm thick antenna substrate at 1.28 GHz, which corresponds with $d/\lambda = 1.7\%$. This antenna is optimized using the proposed strategy to jointly take into account the antenna impedance matching and its circular polarization, expressed by the axial ratio (AR). Afterwards, different antenna prototypes are fabricated using a foam antenna substrate with variable dielectric properties and subsequently optimized to accommodate for the substrate deviations.

This paper is organized as follows. In Section 2, the Galileo E6-band antenna and its requirements are described. In Section 3, the proposed dedicated design strategy is sketched.

2. Aperture-Coupled Galileo E6-Band Antenna

GNSS (global navigation satellite system) services for civil protection can benefit greatly from wearable technology. To extend the functionality of wearable satellite based positioning systems, which usually rely on reception of E1/L1-band signals, we propose a compact, wearable textile antenna intended for Galileo signal reception in the E6-band. In terms of specifications, this means that the antenna has to cover a frequency range from 1.26 to 1.3 GHz. In this range, an $|S_{11}|$ lower than -10 dB is enforced, as well as an AR not exceeding 3 dB, in order to ensure right-hand circular polarization. This antenna is designed for integration into rescue-worker garments. This requires a module that is not only compact and flexible, minimizing hindrance of the wearer's range of motion, but also robust, guaranteeing stable performance in harsh conditions. In order to achieve the above-listed requirements, an aperture-coupled microstrip patch topology, as shown in Figure 1, has been selected. This topology is low profile and the ground plane shields the antenna from the body, reducing its influence on the radiation performance. The aperture coupling reduces the number of vias in the design, increasing robustness to stress occurring when the antenna is bent or compressed. To achieve circular polarization, a Minicircuits QCN-19 [19] discrete hybrid coupler was selected, on the one hand providing a robust circular polarization over a wide frequency range compared to other techniques involving deforming the feed and/or radiating structure, and, on the other hand, leveraging a compact feed circuit, leaving space for the integration of additional electronics on the antenna backside and reducing the vulnerability of the feed circuit to bending influences. The wide-band AR characteristic makes the antenna robust against potential frequency shifts incurred by the integration of the antenna into a garment, exposing it to bending and body proximity. The antenna (excluding a small part of the feed network before the quadrature hybrid) is diagonally symmetrical, as indicated in Figure 1. As a starting point for the Galileo E6-band antenna, we relied on the antenna topology described in [1]. First, the antenna dimensions were rescaled to implement antenna operation in the 1.26 to 1.3 GHz frequency range. Next, the antenna substrate was modified, in the process reducing the substrate height by half. Moreover, a smaller hybrid coupler was applied, as the bulky discrete component used in [1] easily breaks or causes abrasion when inside a jacket in real operating conditions. Both measures enable easier and more comfortable integration into a garment, but they reduce the antenna bandwidth. In order to still meet the requirements, the antenna bandwidth was first enlarged by extending the feed line stubs along the diagonal. Second, the feed structure, together with the patch dimensions, is optimized by means of a Pareto multiobjective optimization to maximize the impedance and axial ratio bandwidth, as described in the next section.

Specifically, the materials used in the construction of this antenna are as follows: for the antenna substrate, a closed-cell expanded rubber foam ($h_1 = 3.94$ mm, $\epsilon_r = 1.56$, $\tan\delta = 0.02$) that is fire-retardant; for the feed substrate, aramid fabric ($h_2 = 400\,\mu$m, $\epsilon_r = 2.15$, $\tan\delta = 0.02$), commonly

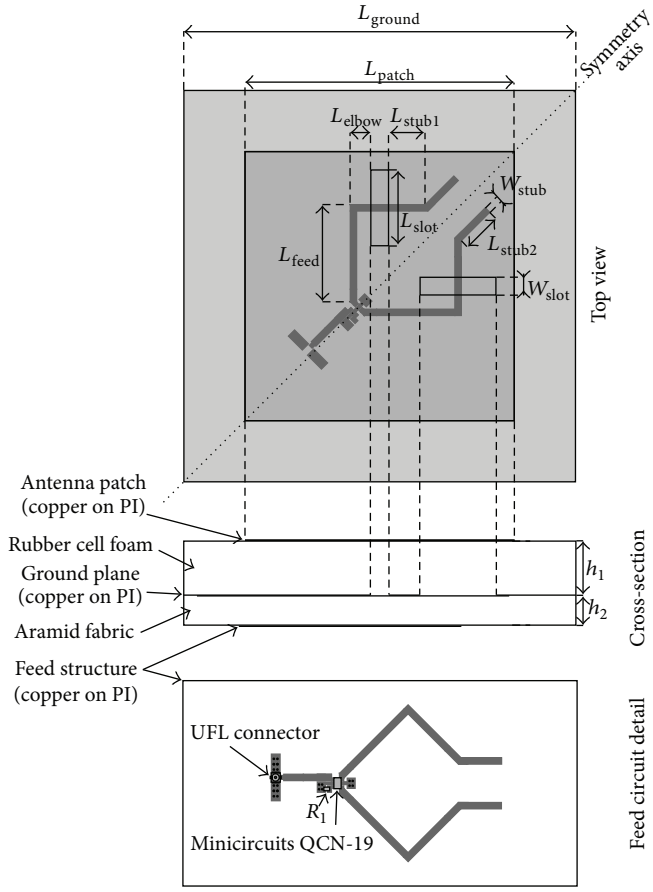

Figure 1: Topology of the E6-band Galileo antenna.

found as an outer layer in protective garments; and for the conductors, copper-on-polyimide (Cu-PI) film, offering good flexibility and robustness, while allowing an accurate manufacturing process by means of photolithography. The Cu-PI film is a laminate of an 18 μm copper layer onto a 50 μm polyimide carrier. This laminate is sourced and processed by the Centre for Microsystems Technology (CMST), Technologiepark, Zwijnaarde. Of these materials, deviations in the dielectric properties of the antenna substrate have the highest effect on the performance of the manufactured prototype, inducing shifts in the antenna frequency response. The significant geometrical parameters for optimization of the antenna performance are the patch length L_{patch}, the slot width W_{slot}, the slot length L_{slot}, and the stub length L_{stub2}. The patch length L_{patch} controls the resonance frequency of the microstrip patch, the slot dimensions W_{slot} and L_{slot} are used to tune the coupling between the feed lines and the patch, and the length of diagonal extension of the feed stubs L_{stub2} is varied to ensure good matching of the antenna to the 50 Ω hybrid coupler. Parameter sweeps, carried out during early design space exploration, show the conflicting nature of the optimization of the antenna bandwidth, on the one side, and the AR, on the other side. While the antenna patch dimensions generally determine the frequency range in which the antenna will operate, increasing the slot dimensions, for example, increases the bandwidth of the antenna by providing a better coupling from the feed lines to the patch at the lower frequencies, but, at the same time, it decreases the AR performance at these frequencies. Increasing the feed line stub length improves the AR performance but, at the same time, decreases the bandwidth. The simultaneous optimization of these parameters is necessary to achieve a right-hand circularly polarized antenna that optimally performs within the Galileo E6-band. In addition, the textile antenna should exhibit sufficient antenna gain in the broadside direction, together with a broad main beam. Yet, the preliminary design process demonstrated that this figure of merit does not critically depend on the antenna design parameters, when considering antenna operation close to an antenna resonance. Therefore, the gain was not added as an additional objective function in the optimization process. Instead, it was verified after the optimization process that the antenna gain indeed exceeds 3 dBi along broadside.

3. Dedicated Multiobjective Constrained Pareto Optimization Strategy

In Figure 2, the dedicated optimization scheme is outlined. At the start, a genetic multiobjective optimizer [20] is used to construct a set of Pareto-optimal solutions in terms of $|S_{11}|$ and AR, relying on a suitable combination of simulation tools.

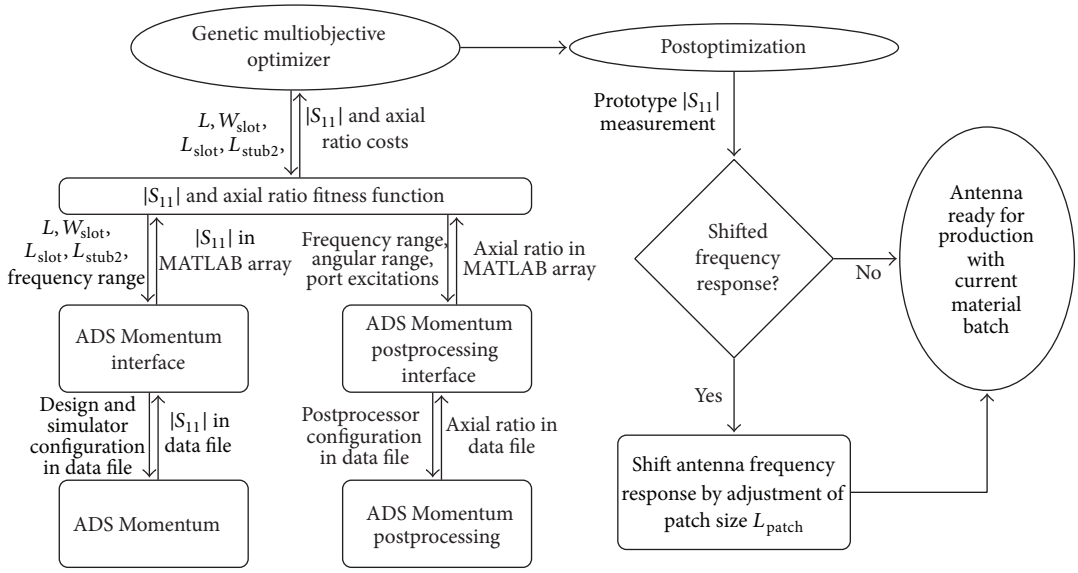

Figure 2: Dedicated optimization scheme for the design of the Galileo E6-band antenna.

Specifically, the SPEA2 algorithm [21] is applied, with a population size of 600 for 200 generations. After this optimization, a final postoptimization step is applied by measuring the $|S_{11}|$ of a first prototype, allowing a final adjustment to take into account deviations occurring between different material batches of the antenna's protective foam substrate.

3.1. Genetic Multiobjective Optimization. In the first step of the optimization strategy, a genetic optimizer is used to avoid getting stuck in local minima in the large design space. To calculate the fitness functions in terms of $|S_{11}|$ and AR, we rely on Agilent's Advanced Design System (ADS) Momentum and the ADS Momentum postprocessing environment, respectively, using interfaces to pass the data from and to MATLAB in a suitable format. The $|S_{11}|$ and AR cost functions are defined by

$$\begin{aligned} \text{cost}_{|S_{11}|} &= \sum_i \left[|S_{11}(f_i)| - |S_{11,\text{lim}}| \right] \\ \text{cost}_{\text{AR}} &= \sum_i \sum_j \left[\text{AR}(f_i, \theta_j) - \text{AR}_{\text{lim}} \right]. \end{aligned} \tag{1}$$

For the $|S_{11}|$ cost function, the limit $|S_{11,\text{lim}}|$ was set to -12 dB from 1.26 GHz to 1.3 GHz. Since the hybrid coupler we intend to use is matched to 50 Ω over a broad frequency range, we do not include it in the optimization of the antenna $|S_{11}|$, because it could hide the reflection characteristics of the antenna itself. For the AR, a limit of $\text{AR}_{\text{lim}} = 2$ dB was imposed for an elevation angle ranging from -30° to 30° in the frequency range from 1.26 GHz to 1.3 GHz, with a 20 MHz step size. To keep the simulation time low, this step size was not chosen smaller, because every frequency at which the AR should be calculated requires an explicit simulation of the antenna structure. For optimization, the antenna's geometrical parameters are allowed to vary within the following ranges:

$$\begin{aligned} &80\text{ mm} < L_{\text{patch}} < 90\text{ mm} \qquad 4\text{ mm} < W_{\text{slot}} < 8\text{ mm} \\ &20\text{ mm} < L_{\text{slot}} < 30\text{ mm} \qquad 10\text{ mm} < L_{\text{stub2}} < 25\text{ mm}. \end{aligned} \tag{2}$$

The antenna structure is simulated using the ADS Momentum planar 3D full-wave EM-solver available in Agilent's ADS 2009. This solver allows efficient calculation of the planar microstrip patch antenna's characteristics, speeding up the optimization process. For the evaluation of the AR, the ADS Momentum postprocessor is used. Reusing the simulation data from the ADS Momentum simulator allows a quick calculation of the AR. The reason we combine two ADS simulation tools with an external optimizer and not with the built-in ADS optimizer is that the ADS optimizer does not allow automatic optimization of the far-field properties of the antenna. By using our dedicated optimization scheme, manual optimization of two conflicting antenna characteristics is circumvented, and the efficient ADS Momentum electromagnetic full-wave field solver can be used for a comprehensive antenna optimization, producing the Pareto front shown in Figure 3. This Pareto front has been constrained using the design requirements for the E6-band antenna put forward in Section 2, being $|S_{11}| < -10$ dB and AR < 3 dB from 1.26 GHz up to 1.3 GHz. The green circles indicate the solutions for which both the $|S_{11}|$ and AR constraints are fulfilled. From these Pareto-optimal points, we have selected the design with the lowest AR error as the final optimal solution. It was verified that, for the selected design, the measured and simulated antenna gains in broadside exceed 3 dBi, with a 3 dB beamwidth larger than 60°, in the complete band of operation. The dimensions of the optimal antenna are given in Table 1.

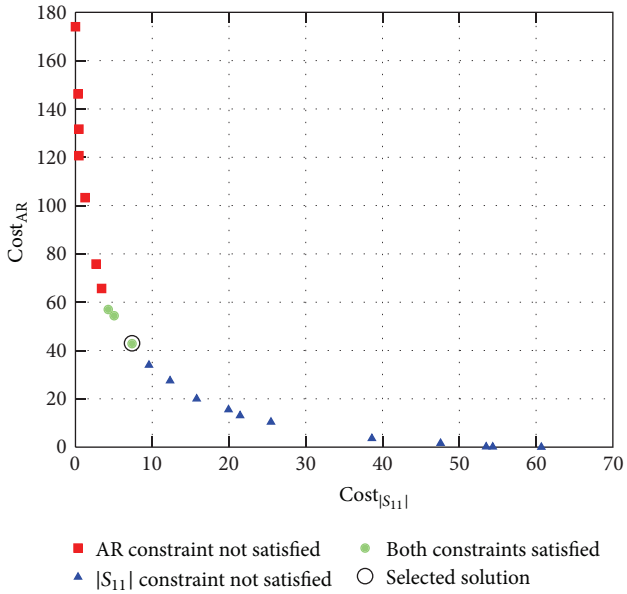

Figure 3: Constrained Pareto front resulting from the E6-band antenna optimization (constraints imposed: AR < 3 dB and $|S_{11}|$ < −10 dB).

Table 1: Dimensions of the optimized antenna.

Parameter	Value [mm]
L_{patch}	84.6415
L_{slot}	24.772
W_{slot}	5
L_{stub1}	9.125
L_{stub2}	18.3626
W_{stub}	1.6
L_{elbow}	5

3.2. Postoptimization Step. The second step in the optimization strategy takes into account the variations on the characteristics of the antenna substrate materials. To this aim, a prototype is constructed using substrate material from a specific material batch. If the dielectric constant of the antenna substrate material deviates from the value applied in the design process, a shift in the antenna's frequency response is noticed. A cost- and time-effective postoptimization step is implemented that takes this material variation into account. The technique consists of slightly varying the antenna patch size to compensate for the induced frequency shift. The patch is a simple structure that is quickly manufactured and replaced on an existing prototype. To illustrate this postoptimization step, the optimized antenna was fabricated using antenna substrate foam from two different batches. The fabrication process for both prototypes is the same. The feed layer conductors are defined by means of a specialized photolithographic process for Cu-PI FCBs (flexible circuit boards). The feed circuit is then laminated onto the aramid fabric feed substrate and laser-cut to the desired shape. The antenna ground plane and patch are laser-cut. Making use of accurately defined alignment holes and a custom

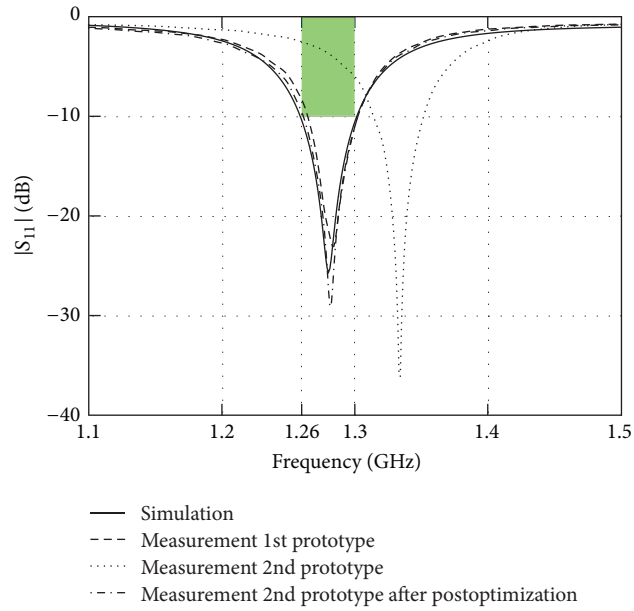

Figure 4: Simulated $|S_{11}|$ (without hybrid coupler) of the optimized Galileo E6-band antenna, together with the −10 dB limit specified by the design requirements (green).

alignment fixture, the different layers are aligned and glued together by means of a thermally activated adhesive sheet to assemble the complete antenna. The performance of the antenna prototypes is measured in an anechoic room by means of an Agilent PNA-X N5242A vector network analyzer (VNA).

In Figure 4, the measured $|S_{11}|$ of the prototypes, of which Figure 5 presents the top and bottom views, is depicted, together with the simulated $|S_{11}|$. Note that the $|S_{11}|$ depicted in Figure 4 is the $|S_{11}|$ of the antenna without the hybrid coupler, as pointed out earlier. The $|S_{11}|$ of the first prototype agrees well with the simulated $|S_{11}|$, whereas the $|S_{11}|$ from the second prototype differs from the simulations. Based on this $|S_{11}|$ measurement, an estimation of the deviation of the dielectric constant of the second material batch is made, and subsequently a new patch size is determined. Compared to the ϵ_r of 1.56 that was used in the first stage of the design, the second substrate material batch exhibits an ϵ_r of 1.46. This is compensated by assembling the second prototype with a patch with a size of 88.2415 mm × 88.2415 mm. The measured $|S_{11}|$ of this final optimized prototype is also depicted in Figure 4.

The simulated and measured AR of the antenna prototypes is depicted in Figure 6, together with the 3 dB limit specified by the design requirements. The postoptimization step significantly improves the performance of the second prototype. In this way, the antennas fabricated using the second material batch also meet the design requirements.

4. Conclusion

A flexible dedicated multiobjective computer-aided optimization scheme is applied to the design of a circularly

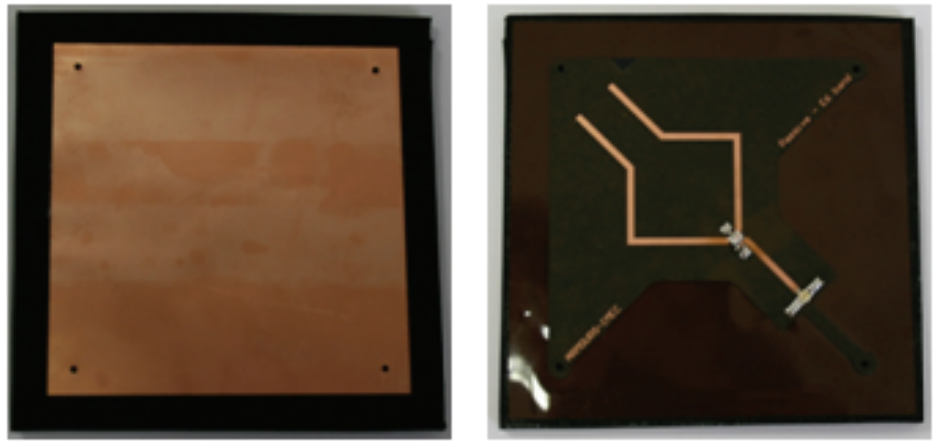

(a) (b)

Figure 5: Back (a) and front (b) of the manufactured Galileo E6-band antenna.

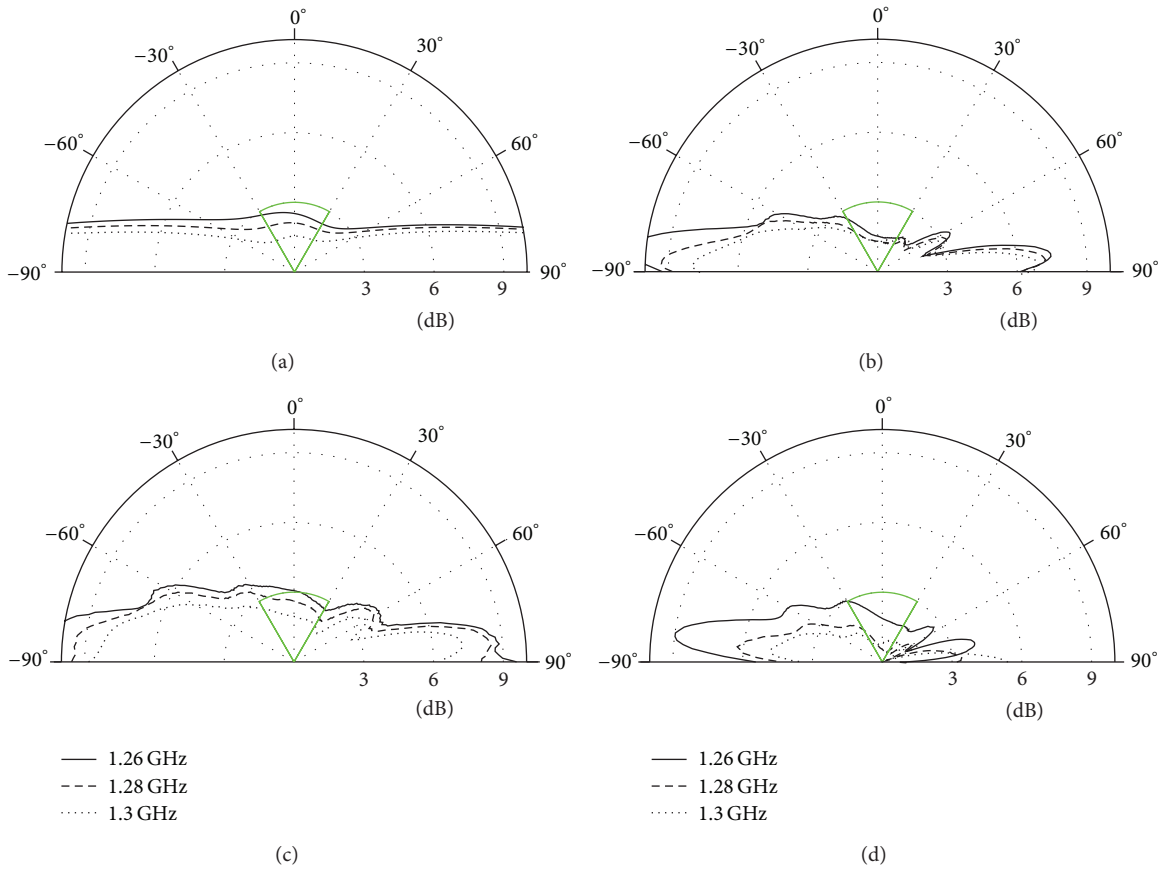

Figure 6: Simulated (a) and measured ((b), (c), and (d): prototype 1, prototype 2 before postoptimization, and prototype 2 after postoptimization, resp.) AR of the Galileo E6-band antenna, together with the 3 dB limit specified by the design requirements (green).

polarized Galileo E6-band antenna, allowing a proprietary design using a genetic multiobjective Pareto optimization linked with appropriately selected simulation tools, together with a material batch-specific postoptimization step consisting of altering the patch size based on a prototype $|S_{11}|$ measurement, to account for variations of the unconventional substrate materials used in the textile antenna design process. The Galileo E6-band antenna is optimized in terms of return loss and AR characteristics. The validity of the strategy and the included postoptimization step is confirmed by means of the construction of two prototypes, using two different batches of antenna substrate material. Both antenna

prototypes (one after applying the postoptimization step to account for the different material batch) meet the design requirements, showing that the proposed optimization strategy is able to efficiently take into account the variations on the antenna substrate material.

Conflict of Interests

The authors declare that there is no conflict of interests regarding the publication of this paper.

Acknowledgment

This work was cofunded by the European Commission in the context of the EC-FP7 Galileo.2011.3.1-2: Collaborative Project, Grant agreement no. 287166.

References

[1] A. Dierck, H. Rogier, and F. Declercq, "A wearable active antenna for global positioning system and satellite phone," *IEEE Transactions on Antennas and Propagation*, vol. 61, no. 2, pp. 532–538, 2013.

[2] A. Dierck, S. Agneessens, F. Declercq et al., "Active textile antennas in professional garments for sensing, localisation and communication," *International Journal of Microwave and Wireless Technologies*, pp. 1–11.

[3] S. Agneessens, P. van Torre, F. Declercq et al., "Design of a wearable, low-cost, through-wall doppler radar system," *International Journal of Antennas and Propagation*, vol. 2012, Article ID 840924, 9 pages, 2012.

[4] J. Lilja, P. Salonen, T. Kaija, and P. de Maagt, "Design and manufacturing of robust textile antennas for harsh environments," *IEEE Transactions on Antennas and Propagation*, vol. 60, no. 9, pp. 4130–4140, 2012.

[5] J. Lilja, V. Pynttäri, T. Kaija et al., "Body-worn antennas making a splash: lifejacket-integrated antennas for global search and rescue satellite system," *IEEE Antennas and Propagation Magazine*, vol. 55, no. 2, pp. 324–341, 2013.

[6] E. K. Kaivanto, M. Berg, E. Salonen, and P. De Maagt, "Wearable circularly polarized antenna for personal satellite communication and navigation," *IEEE Transactions on Antennas and Propagation*, vol. 59, no. 12, pp. 4490–4496, 2011.

[7] G. Orecchini, M. M. Tentzeris, L. Yang, and L. Roselli, "Smart shoe: an autonomous inkjet-printed RFID system scavenging walking energy," in *Proceedings of the IEEE International Symposium on Antennas and Propagation and USNC/URSI National Radio Science Meeting (APSURSI '11)*, pp. 1417–1420, July 2011.

[8] A. A. Serra, P. Nepa, and G. Manara, "A wearable multi antenna system on a life jacket for Cospas Sarsat rescue applications," in *Proceedings of the IEEE International Symposium on Antennas and Propagation (APSURSI '11)*, pp. 1319–1322, July 2011.

[9] Q. Bai and R. Langley, "Crumpling of PIFA textile antenna," *IEEE Transactions on Antennas and Propagation*, vol. 60, no. 1, pp. 63–70, 2012.

[10] F. Boeykens, H. Rogier, and L. Vallozzi, "An efficient technique based on polynomial chaos to model the uncertainty in the resonance frequency of textile antennas due to bending," *IEEE Transactions on Antennas and Propagation*, vol. 62, no. 3, pp. 1253–1260, 2014.

[11] S. Koulouridis, D. Psychoudakis, and J. L. Volakis, "Multiobjective optimal antenna design based on volumetric material optimization," *IEEE Transactions on Antennas and Propagation*, vol. 55, no. 3 I, pp. 594–603, 2007.

[12] S. Koziel and S. Ogurtsov, "Multi-objective design of antennas using variable-fidelity simulations and surrogate models," *IEEE Transactions on Antennas and Propagation*, vol. 61, no. 12, pp. 5931–5939, 2013.

[13] D. Bianchi, S. Genovesi, and A. Monorchio, "Constrained Pareto optimization of wide band and steerable concentric ring arrays," *IEEE Transactions on Antennas and Propagation*, vol. 60, no. 7, pp. 3195–3204, 2012.

[14] T. H. Nguyen, H. Morishita, Y. Koyanagi, K. Izui, and S. Nishiwaki, "A multi-level optimization method using PSO for the optimal design of an L-shaped folded monopole antenna array," *IEEE Transactions on Antennas and Propagation*, vol. 62, no. 1, pp. 206–215, 2014.

[15] C. Gazda, I. Couckuyt, H. Rogier, D. Vande Ginste, and T. Dhaene, "Constrained multiobjective optimization of a common-mode suppression filter," *IEEE Transactions on Electromagnetic Compatibility*, vol. 54, no. 3, pp. 704–707, 2012.

[16] S. K. Goudos and J. N. Sahalos, "Pareto optimal microwave filter design using multiobjective differential evolution," *IEEE Transactions on Antennas and Propagation*, vol. 58, no. 1, pp. 132–144, 2010.

[17] J. Kovitz and Y. Rahmat-Samii, "Using thick substrates and capacitive probe compensation to enhance the bandwidth of traditional cp patch antennas," *IEEE Transactions on Antennas and Propagation*, vol. 62, no. 10, pp. 4970–4979, Oct 2014.

[18] W. L. Langston and D. R. Jackson, "Impedance, axial-ratio, and receive-power bandwidths of microstrip antennas," *IEEE Transactions on Antennas and Propagation*, vol. 52, no. 10, pp. 2769–2773, 2004.

[19] Mini-Circuits, Ultra-Small Ceramic Power Splitter/Combiner, QCN-19 data sheet.

[20] K. Deb, *Multi-Objective Optimization using Evolutionary Algorithms*, Wiley-Interscience Series in Systems and Optimization, John Wiley & Sons, Chichester, UK, 2001.

[21] E. Zitzler, M. Laumanns, and L. Thiele, "SPEA2: improving the strength pareto evolutionary algorithm for multiobjective optimization," in *Evolutionary Methods for Design, Optimisation and Control with Application to Industrial Problems*, pp. 95–100, International Center for Numerical Methods in Engineering, Barcelona, Spain, 2001.